Northumbria Research Link

Citation: Lin, Bangjiang, Xu, Junxiang, Ghassemlooy, Zabih and Tang, Xuan (2019) Power-code division non-orthogonal multiple access scheme for next-generation passive optical networks. Optics Express, 27 (24). pp. 35740-35749. ISSN 1094-4087

Published by: Optical Society of America

URL: https://doi.org/10.1364/oe.27.035740 <https://doi.org/10.1364/oe.27.035740>

This version was downloaded from Northumbria Research Link: http://nrl.northumbria.ac.uk/id/eprint/41599/

Northumbria University has developed Northumbria Research Link (NRL) to enable users to access the University's research output. Copyright © and moral rights for items on NRL are retained by the individual author(s) and/or other copyright owners. Single copies of full items can be reproduced, displayed or performed, and given to third parties in any format or medium for personal research or study, educational, or not-for-profit purposes without prior permission or charge, provided the authors, title and full bibliographic details are given, as well as a hyperlink and/or URL to the original metadata page. The content must not be changed in any way. Full items must not be sold commercially in any format or medium without formal permission of the copyright holder. The full policy is available online: http://nrl.northumbria.ac.uk/policies.html

This document may differ from the final, published version of the research and has been made available online in accordance with publisher policies. To read and/or cite from the published version of the research, please visit the publisher's website (a subscription may be required.)

Northumbria University NEWCASTLE

University Library

Research Article | Vol. 27, No. 24 / 25 November 2019 / Optics Express 35740
Optics EXPRESS

Power-code division non-orthogonal multiple access scheme for next-generation passive optical networks

BANGJIANG LIN,[1] JUNXIANG XU,[1] ZABIH GHASSEMLOOY,[2] AND XUAN TANG[1,*]

[1] *Quanzhou Institute of Equipment Manufacturing, Haixi Institutes, Chinese Academy of Sciences, China*
[2] *Optical Communications Research Group, Faculty of Engineering and Environment, Northumbria University, UK*
[*] *xtang@fjirsm.ac.cn*

Abstract: Advanced modulation and multiple access schemes with high spectral efficiencies are desirable to overcome the bandwidth limitation in low-cost optical and electrical devices to fulfill the high-data rate requirements in passive optical networks (PONs). We propose a non-orthogonal multiple access (NOMA) scheme, known as power-code division NOMA (PCD-NOMA), for the next-generation PON, where the optical network units (ONUs) are divided into several groups with similar path losses. The ONUs per groups are allocated in the same power domain multiplexing layer with different codebooks. We show by experimental demonstration that the proposed PCD-NOMA with a high spectral efficiency offers improved overall system performance and reduced required transmission power in the next-generation PON, particularly in flexible PON where ONUs have different path losses. For PON with a power difference loss of 14 dB, the reduced required transmission powers are 5 and 11 dB for downstream and upstream, respectively, compared with orthogonal frequency division multiple access.

© 2019 Optical Society of America under the terms of the OSA Open Access Publishing Agreement

1. Introduction

The increasing data traffic generated by bandwidth-consuming applications such as high-definition video streaming services and wireless backhaul in 5th generation (5G) networks are setting the mile-stone in the next generation optical network with higher speed, flexibility and reliability [1–5]. Current time division multiple access (TDMA)-based passive optical networks (PONs) are unable to provide data rates higher than 40Gb/s due to chromatic dispersion induced transmission impairments and high complexity of burst-mode transceivers [6]. A number of PON technologies have been proposed to provide future broadband optical access including time- and wavelength-division multiplexing (TWDM)-PON, wavelength division multiple access (WDMA)-PON and orthogonal frequency division multiple access (OFDMA)-PON [7–12]. WDMA-PON, which provides a virtual point-to-point fiber access connection via a dedicated wavelength to each optical network unit (ONU), offers a much higher data rate but at higher costs [9]. OFDMA-PON provides high spectrum efficiency, large dispersion tolerance and high flexibility on multiple services provisioning at the cost of lower power efficiency, which is limited by the high peak to average power ratio (PAPR) [10–12]. In order to avoid or alleviate interference, the above-mentioned PONs adopt the orthogonal multiple access (OMA) scheme, where different optical network unit (ONUs) are allocated to orthogonal resources in either the time or frequency (wavelength) domain.

As one of the key enabling technologies for the physical layer in the next generation wireless communications, non-orthogonal multiple access (NOMA) has received a lot attention from academic and industry [13–16]. In NOMA signals are overlapped in both time and frequency domains, thus offering higher throughput and improved spectral efficiency compared with OMA.

#380168 https://doi.org/10.1364/OE.27.035740
Journal © 2019 Received 11 Oct 2019; revised 5 Nov 2019; accepted 11 Nov 2019; published 20 Nov 2019

Optics EXPRESS

NOMA can be categorized in both power and code domains [13] (i.e., PD-NOMA and CD-NOMA). Users are multiplexed in power domain by assigning distinct power levels to different users [14] and in code domain using user-specific spreading sequences [15] for PD-NOMA and CD-NOMA, respectively. Recently, PD-NOMA was proposed to increase the spectrum efficiency of coherent optical OFDM systems [17]. Both PD-NOMA and CD-NOMA schemes were proposed to address the bandwidth limitation of visible light communications (VLC) systems [18–22]. PD-NOMA was shown to be particularly suitable for indoor VLC systems and has been widely investigated.

In previous works, applications of PD-NOMA [23] and CD-NOMA [24] in PONs were experimentally demonstrated offering twice and 150% the data rate compared with OFDMA using the same bandwidth, respectively. Note, PD-NOMA can achieve improved sum rate in the case where the users experience different path losses (i.e., different signal to noise ratios (SNRs) at the receiver (Rx)). In PON, ONUs are connected to the optical line terminal (OLT) via an optical distribution network (ODN), which have different path losses depending on the distances between ODN and ONUs. For a PON system with a coverage length of 100 km, the maximum path loss difference (PLD) is 20 dB assuming that the fiber attenuation coefficient is 0.2 dB/km. In [25], a multi-stack structure based ODN, where the new subscribe is connected to the closet connected ONU via a coupler, which is low cost and highly flexible, is proposed to expand the network. As such, the connected users in the network experience quite different path losses. In the OMA scheme, it is challenging to provide high-speed services to the entire ONUs since the service quality is mostly affected by the ONU with the largest path loss. In [25], the PD-NOMA scheme with synchronized downlink and asynchronous uplink was proposed to improve the performance and reliability of the flexible PON.

In this paper, we extended our previous works [23,24] and propose a new NOMA scheme known as power-code division NOMA (PCD-NOMA) for the next generation PON, where ONUs are divided into a number of groups with ONUs in the same group with similar path losses and in the same power domain multiplexing layer (PDML) are allocated with different codebooks. At the Rx, the successive interference cancellation (SIC) together with the message passing algorithm (MPA) is used to remove the inter-user interference (IUI). Compared with OMA and other NOMA schemes, PCD-NOMA offers higher spectral efficiency and sum rate. We show by experimental demonstration that, PCD-NOMA can significantly improve the performance and reliability for the ONU with a higher path loss by adjusting the power allocation ratio adaptively, thus improving the overall system performance and reducing the required transmit optical power P_{Tx}.

2. Technique principle

Figure 1 shows the architecture of flexible PON with a multi-stack structure. Note, (*i*) the existing TDMA-PON infrastructure can be reused and the new subscribers can be added via a coupler to the closet connected ONU; (*ii*) the downstream data is broadcast to all ONUs; and (*iii*) the ONUs in the same group have similar received optical power (ROP) (i.e., similar SNR), which is not the same in in different groups. A two-dimensional resource allocation in both code and power domains with N power domain multiplexing layers (PDMLs) and C codebooks is also illustrated in Fig. 1. Note, in terms of dynamic resource allocation PCD-NOMA is compatible with TDMA and OFDMA. In the proposed PCD-NOMA, the ONU group with the highest link loss is allocated with the largest power in the PDML domain and ONUs within the same group are allocated with different codebooks.

Figure 2 shows the system block diagram for the downstream PCD-NOMA PON system with M subcarriers, C code-books and N PDMLs. The same code-books are used in different PDML. At the transmitter (Tx), all source data in the n^{th} PDML are directly mapped to the multi-dimensional codewords (i.e., $\mathbf{X^n_1}$, $\mathbf{X^n_2}$, ..., $\mathbf{X^n_C}$), respectively. Note that, $\mathbf{X^n_c} = [X^n{}_{1,c},$

Optics EXPRESS

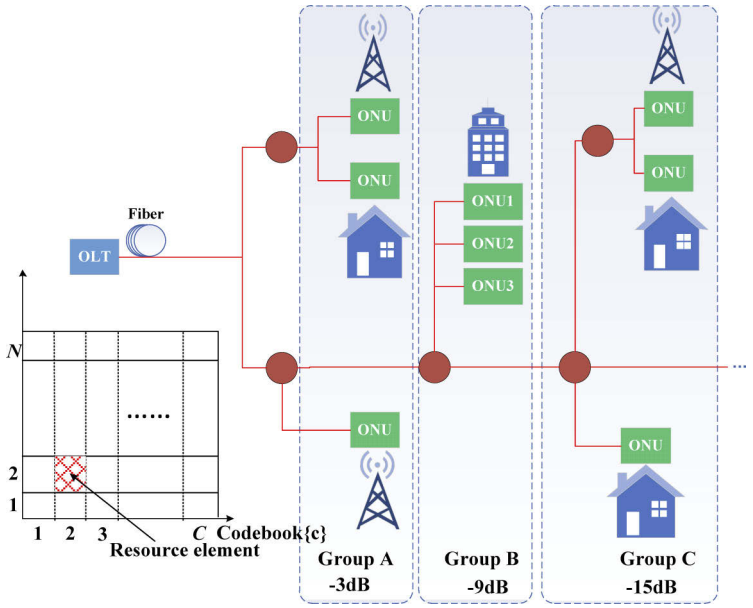

Fig. 1. Flexible PON with uneven path losses.

$X^n{}_{2,c}, \ldots, X^n{}_{M,c}]^T$, where $1 < c < C$. The combined C codewords are spread over M frequency resources (i.e., OFDM subcarriers). In order to generate a real value signal Hermitian symmetry is applied prior to inverse discrete Fourier transform (IDFT). For each OFDM symbol cyclic prefix (CP) and preamble are added to combat the chromatic dispersion induced inter-symbol interference (ISI) and provide synchronization and channel estimation, respectively. Following power allocation, signals at different PDMLs are added together. The transmitted signal for the m^{th} subcarrier ($m = 1, \ldots, M$) in the frequency domain is given by:

$$X_m = \sum_{n=1}^{N} \sqrt{p_n} \sum_{c=1}^{C} X^n{}_{m,c}, \tag{1}$$

where p_n is the allocation power for n^{th} PDML. Note, power allocation is realized in the digital and power domains for downstream and upstream, respectively. PDML with the highest index is allocated with the lowest power. The combined signal is applied to a digital-to-analog converter (DAC) prior to external modulation (EM) of the laser source for transmission over the single mode fiber (SMF).

The transmitted data are broadcast to all ONUs but at different SNR levels as shown in Fig. 1. In each ONU, following optical to electrical detection the output of the Rx is applied to an analog-to-digital converter (ADC). Following frame synchronization and CP removal the received signal for the 1st PDML is given by:

$$\mathbf{Y^1} = \sum_{n=1}^{N} \sqrt{p_n} \sum_{c=1}^{C} \mathbf{h}\mathbf{X}^{\mathbf{n}}{}_{\mathbf{c}} + \mathbf{n}, \tag{2}$$

where $\mathbf{h}$ denotes the channel response matrix and $\mathbf{n}$ is the additive white Gaussian noise (AWGN). $\mathbf{h} =$ diag $(H_1, H_2, \ldots, H_M)$ and $\mathbf{n} = [n_1, n_2, \ldots, n_M]^T$, where H_{m} and n_m denote the channel response and the AWGN for the m^{th} subcarrier, respectively. Following discrete Fourier transform (DFT) and channel equalization (CE) (i.e., $\mathbf{Y^1}$ is divided by $\sqrt{p_1}\mathbf{H}$) the received signal for the

Optics EXPRESS

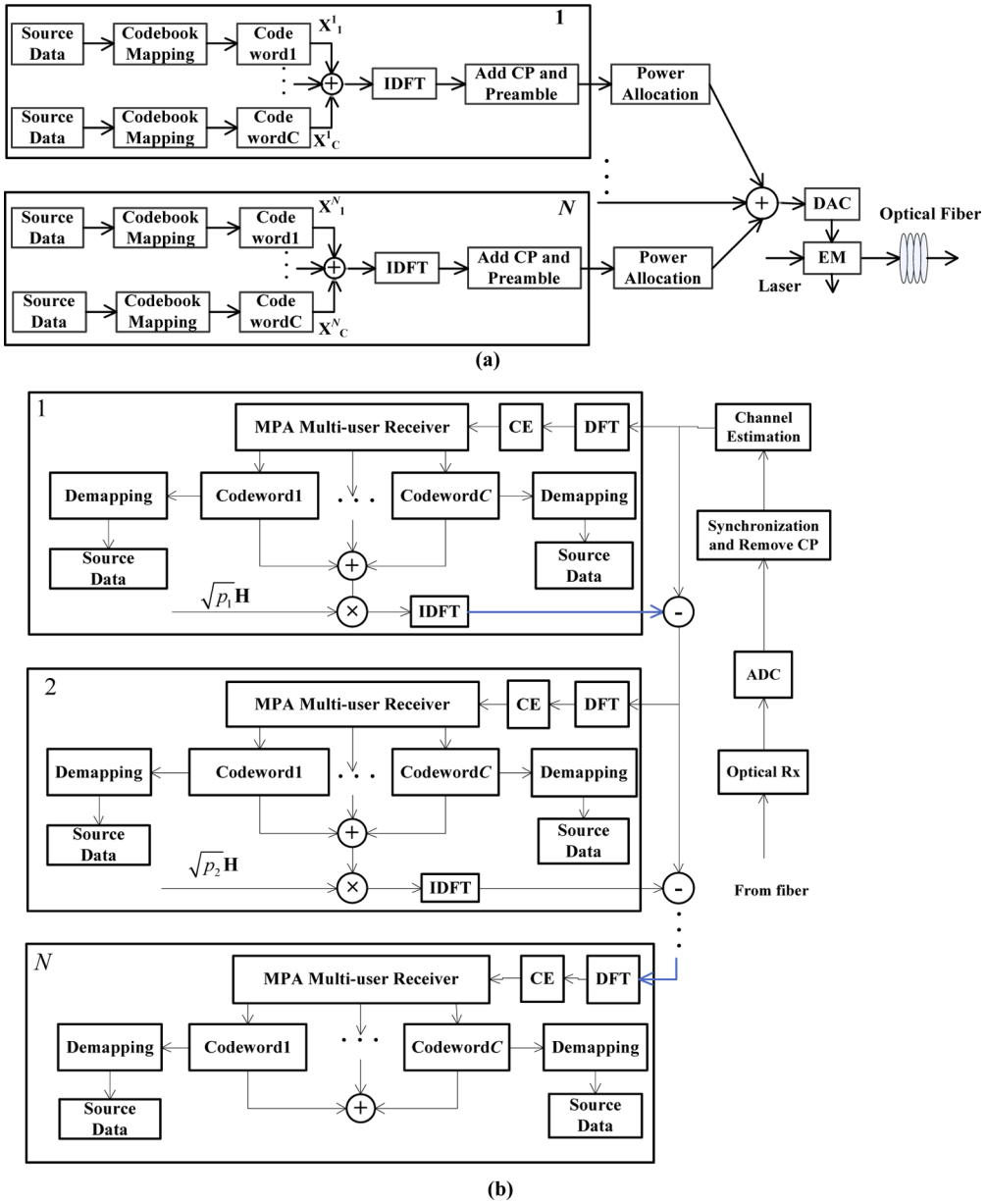

Fig. 2. Block diagram of downstream PCD-NOMA PON: (a) the transmitter and (b) the receiver.

Optics EXPRESS

m^{th} subcarrier is given as:

$$Y^1{}_m = \sum_{c=1}^{C} X^1{}_{m,c} + \sum_{n=2}^{N} \sqrt{\frac{p_n}{p_1}} \sum_{c=1}^{C} X^n{}_{m,c} + \frac{n_m}{\sqrt{p_1} H_m}. \tag{3}$$

where $\mathbf{H} = [H_1, H_2, \ldots, H_M]^T$. The second term in (3) is the IUI.

Next, the equalized signal is applied to the MPA Rx, see Fig. 1(b), the output of which is applied to codeword modules to recover data sources via demapping for the 1$^{\text{st}}$ PDML. The combined cod-words are scaled by $\sqrt{p_1}\mathbf{H}$ prior to being applied to the IDFT module. Next, the received signal for the 2$^{\text{nd}}$ PDML at the output of DFT is given as:

$$\mathbf{Y^2} = \sum_{n=2}^{N} \sqrt{p_n} \sum_{c=1}^{C} \mathbf{h} \mathbf{X^n_c} + \mathbf{n}, \tag{4}$$

Note that, $\mathbf{Y^2} = [Y^2{}_1, Y^2{}_2, \ldots, Y^2{}_M]^T$. Following CE, the received signal for the m^{th} subcarrier, which is divided by $H_m\sqrt{p_2}$, is given as:

$$Y^2{}_m = \sum_{c=1}^{C} X^2{}_{m,c} + \sum_{n=3}^{N} \sqrt{\frac{p_n}{p_2}} \sum_{c=1}^{C} X^n{}_{m,c} + \frac{n_m}{\sqrt{p_2} H_m}. \tag{5}$$

Similarly, the received signal for the m^{th} subcarrier for the N^{nd} PDML is given by:

$$Y^N{}_m = \sum_{c=1}^{C} X^N{}_{m,c} + \frac{n_m}{\sqrt{p_n} H_m}. \tag{6}$$

Note, in PCD-NOMA, MPA and SIC Rxs are applied N and $(N-1)$ times, respectively in order to decode all the transmitted signals. The total system complexity is defined as:

$$o\,(NI_T|\pi|^d + (N-1)\frac{M}{2} log_2 M), \tag{7}$$

where π is the codebook set size, I_T denotes the number of iterations for each MPA Rx and d represents the non-zero elements in each row of the factor graph matrix.

3. Experiment setup and results

In this section, we investigate transmission performance of the proposed PCD-NOMA PON, using the experimental setup shown in Fig. 3. The numbers of codebooks and PDML are 6 and 2 (i.e., $C = 6$, $N = 2$), respectively. Note, the codebooks adopted in this work can be found in [24]. At OLT, the generated codewords from the 6 data sources are superposed and spread over 4 subcarriers, see Fig. 2(a). The number of subcarriers is 256 of which 120 subcarriers are used for data transmission. The output of the PCD-NOMA coder module is uploaded to an arbitrary waveform generator (AWG, Tektronix 70002A) with a sampling rate of 10 GS/s, the output of which is used for EM of a laser using a Mach-Zehnder modulator (MZM). The output of the MZM is fed into a 20 km long SMF via an optical circulator. The ODN is emulated using a 50/50 optical coupler and a variable optical attenuator, thus ensuring two ONUs having different ROP. The ONU with higher path loss is allocated with a higher power level. At ONU, an optical Rx (composed of a photodetector (PD) and an electrical amplifier (EA) with 20 dB gain and ~8GHz bandwidth) is used to regenerate the electrical signal, which is captured by a digital oscilloscope (Tektronix DPO71604C, 16GHz bandwidth and maximum sampling rate of 100GS/s) with a sampling rate of 25 GS/s. The capture signal is processed (i.e., decoded) using MPA-SIC Rx to

Optics EXPRESS

recover the transmitted data, see Fig. 2(b). In the upstream, the OFDM signals applied to AWG are used for EM of the laser sources for transmission over a SMF via ODN to the OLT. Note, the power allocation ratio between the two ONUs depends on the PLD. The PLD can be adjusted by changing the transmit powers of the two lasers. At OLT, the output of the optical Rx is captured by a scope for post processing using a MPA-SIC Rx. All the key system parameters are provided in Table 1.

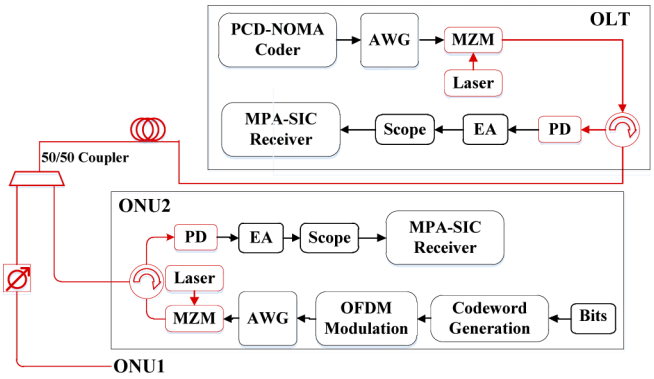

Fig. 3. Experimental setup for PCD-NOMA PON with two ONUs.

Figure 4 show the bit error rate (BER) as a function of the ROP for the downstream PCD-NOMA-VLC for ONUs 1 and 2 and for a range of power allocation ratios (PAR). ONU1, which has a higher path loss compared with ONU2, is allocated with a higher power level. Also shown for comparison are the BER plots for OFDM and CD-NOMA PON links, where CD-NOMA offers the best performance compared with all cases. Note that, (*i*) the number of iterations for each MPA Rx was set to 4, which is optimized in the experiment considering the tradeoff between complexity and performance; (*ii*) the signal to interference plus noise ratio (SINR) for ONU1 decreases with the increase in PAR. As shown in Fig. 4, ONU1 displays improved BER performance compared with ONU2 for all values of PAR. However, the lowest BERs are observed for the PAR values of 0.01 and 0.04 for ONUs 1 and 2, respectively. At the 7% hard-decision forward error correction (HD-FEC) BER limit of 3.8×10^{-3} we observe the followings: (*i*) the Rx's sensitivity ranges for ONU 1 and 2 are −17 to −15 dBm and −9 to −5 dBm, respectively, −17.5 and −10 dBm for CD-NOMA and OFDMA, respectively; (*ii*) compared with the CD-NOMA the power penalties are 0.5, 1 and 2.6 dB for the PAR values of 0.01, 0.023 and 0.04 for ONU1 increasing to 12.5, 10 and 8.5 dB for ONU2, respectively. In practical applications, PAR should be optimized by considering the specific power loss difference between ONUs. In general, higher power loss differences are associated with the lower PAR values. In OMA, the ONU with the largest path loss has the worst BER performance, thus limiting the overall system performance, whereas in PCD-NOMA ONUs can offer similar BER performance by means of a fair power allocation policy. In OFDMA, to achieve the same data rate compared with PCD-NOMA using the same bandwidth, 64-QAM mapping is used. Note, the Baud rates and bandwidth utilization ratios for all schemes are 5 Gaud and 45.5%, respectively. In the downstream link, all the ONUs have the same Rx sensitivity for CD-NOMA and OFDMA. PCD-NOMA offers twice the data rate at the cost of reduced Rx's sensitivity for both ONUs compared with CD-NOMA since the codebook is reused twice. Table 2 shows the required P_{Tx} at the OLT to maintain the BER values below the 7% HD-FEC limit for OFDMA and PCD-NOMA for a PAR of 0.04. For ONU2, the path loss is fixed at 7 dB whereas for ONU1 the path loss is variable set by the optical attenuator. The required P_{Tx} for OFDMA increases with the path loss of ONU1, and for PCD-NOMA it depends on the path loss of ONU2 for PLD $<$ 5 dB and ONU1

Optics EXPRESS

Table 1. System parameters

Parameter	Value
Total data rate	
PCD-NOMA and OFDMA	13.6 Gbps
CD-NOMA	6.8 Gbps
No. of subcarriers – All 3 schemes	120
DFT and CP – All 3 schemes	256 and 8
Modulation - OFDM	64-QAM
No. of codewords – PCD-NOMA & CD-NOMA	6
MZM	
3 dB bandwidth	10 GHz
Half-wave voltage	4.6 V
Insertion Loss	3.2 dB
Bias voltage	2.5 V
Operating wavelength	1525-1565 nm
Distributed feedback laser	
Wavelength	1550 nm
Downstream power	0 dBm
Upstream power	−15 - 0 dBm
SMF	
Length	20 km
Dispersion	16e-6 s/m^2
Loss	0.2 dB/km
Optical Rx	
PD's responsibility@1550nm	0.87 A/W
Bandwidth	10 GHz
Gain of amplifier	20 dB
Dark current	10.5 nA

for PLD > 5 dB. Therefore, PDC-NOMA can reduce the required P_{Tx}. In addition, the required P_{Tx} can be reduced by adjusting the PAR adaptively in the digital domain.

Table 2. The required transmit power in downstream

PLD (dB)	PCD-NOMA (dBm)	OFDMA (dBm)
3	−3	0
4	−3	1
5	−3	2
6	−2	3
7	−1	4
8	0	5
9	1	6

Figure 5 depicts the upstream BER performance against the P_{Tx} for PCD-NOMA for ONUs 1 and 2 and for a PLD of 14 dB. Note, P_{Tx} (i.e., output power from MZMs) for both ONUs are kept the same. As shown, ONU1 display the worth BER compared with ONU2 since it has a higher

Optics EXPRESS

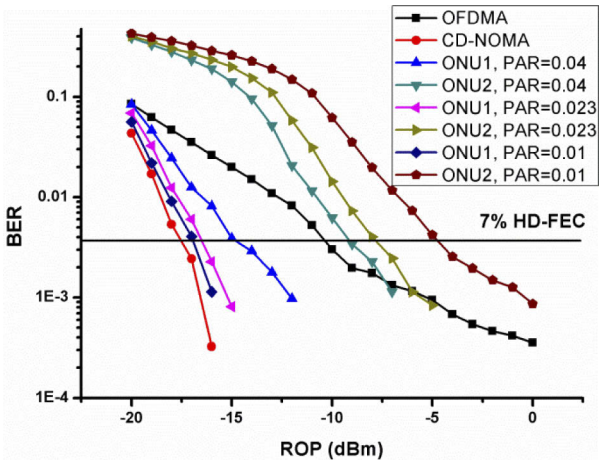

Fig. 4. Measured BER as a function of ROP for downstream PON with two ONUs.

path loss. At the 7% HD-FEC BER limit, the power penalty is −3 dB for ONU1 compared with ONU2. As shown in Fig. 5, the required transmit optical power is about −3 dBm for PDC-NOMA to ensure all the BER is below the 7% HD-FEC limit. Assuming that for the upstream link the Rx's sensitivity is the same as that of the downstream link, the required P_{Tx} is 8 dBm for OFDMA in order to ensure that BER values are below the 7% HD-FEC limit. Note, compared with OFDMA, PCD-NOMA offers higher complexity particularly in the receiver side as shown in (7). It is challenging to further increase the number of PDML due to high user interference. More advanced receiver is required to reduce or remove the inter-user interferences.

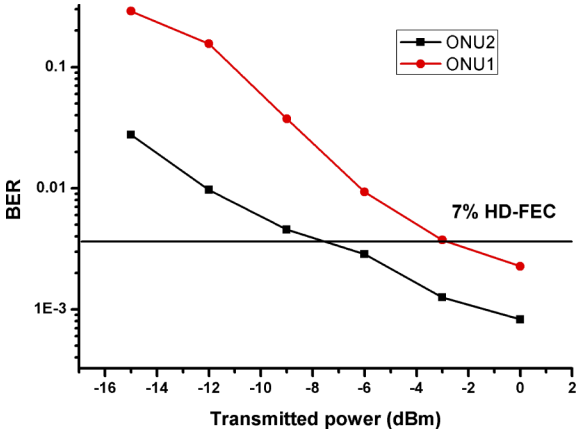

Fig. 5. Measured BER as a function of transmit power for upstream PCD-NOMA PON with a PLD of 14 dB.

4. Conclusions

We proposed PCD-NOMA for the next generation PON, which used both code and power domains to transmit multiple users' signals over a subcarrier simultaneously and a SIC-MPA receiver to remove the inter user interference. Compared with OMA and other NOMA schemes, PCD-NOMA offered higher spectrum effiency. We showed by experimental investigation that, PCD-NOMA offered improved perofrmance and reliablity of ONU with a higher path loss by

Optics EXPRESS

adjusting the power allocation ratio adaptively. With the reduced transmit optical power and improved overall systme performance, PCD-NOMA could be used to overcome the bandwidth limitation of optical and eletrical devices in the next genaration PON, particularly in flexible PONs with ONUs having different path losses.

Funding

National Natural Science Foundation of China (61601439); Natural Science Foundation of Fujian Province (2017J05111).

Acknowledgments

The authors would like to thank Professor Zhangyuan Chen and Juhao Li from Peking University for the support of open funding and experimental testbed.

Disclosures

The authors declare no conflicts of interest.

References

1. Z. Zhu, W. Lu, L. Zhang, and N. Ansari, "Dynamic Service Provisioning in Elastic Optical Networks with Hybrid Single-/Multi-Path Routing," J. Lightwave Technol. **31**(1), 15–22 (2013).
2. L. Gong and Z. Zhu, "Virtual Optical Network Embedding (VONE) over Elastic Optical Networks," J. Lightwave Technol. **32**(3), 450–460 (2014).
3. L. Gong, X. Zhou, X. Liu, W. Zhao, W. Lu, and Z. Zhu, "Efficient Resource Allocation for All-Optical Multicasting over Spectrum-Sliced Elastic Optical Networks," J. Opt. Commun. Netw. **5**(8), 836–847 (2013).
4. P. Lu, L. Zhang, X. Liu, J. Yao, and Z. Zhu, "Highly-Efficient Data Migration and Backup for Big Data Applications in Elastic Optical Inter-Data-Center Networks," IEEE Netw. **29**(5), 36–42 (2015).
5. Y. Yin, H. Zhang, M. Zhang, M. Xia, Z. Zhu, S. Dahfort, and S. J. B. Yoo, "Spectral and Spatial 2D Fragmentation-Aware Routing and Spectrum Assignment Algorithms in Elastic Optical Networks," J. Opt. Commun. Netw. **5**(10), A100–A106 (2013).
6. C. Li, J. Chen, Z. Li, Y. Song, Y. Li, and Q. Zhang, "Demonstration of symmetrical 50-Gb/s TDM-PON in O-band supporting over 33-dB link budget with OLT-side amplification," Opt. Express **27**(13), 18343–18350 (2019).
7. Z. Tan, C. Yang, and Z. Wang, "Energy Consume Analysis for Ring-Topology TWDM-PON Front-Haul Enabled Cloud RAN," J. Lightwave Technol. **35**(20), 4526–4534 (2017).
8. Z. Tan, C. Yang, and Z. Wang, "Energy Evaluation for Cloud RAN Employing TDM-PON as Front-haul Based on a New Network Traffic Modeling," J. Lightwave Technol. **35**(13), 2669–2677 (2017).
9. K. Matsuda, R. Matsumoto, and N. Suzuki, "Hardware-Efficient Adaptive Equalization and Carrier Phase Recovery for 100-Gb/s/λ-Based Coherent WDM-PON Systems," J. Lightwave Technol. **36**(8), 1492–1497 (2018).
10. T. Wu, C. Zhang, H. Wei, and K. Qiu, "PAPR and security in OFDM-PON via optimum block dividing with dynamic key and 2D-LASM," Opt. Express **27**(20), 27946–27961 (2019).
11. J. Zhang, C. Guo, J. Liu, X. Wu, A. P. Lau, C. Lu, and S. Yu, "Decision-Feedback Frequency-Domain Volterra Nonlinear Equalizer for IM/DD OFDM Long-Reach PON," J. Lightwave Technol. **37**(13), 3333–3342 (2019).
12. H. Y. Chen, C. C. Wei, C. Y. Lin, L. W. Chen, I. C. Lu, and J. Chen, "Frequency-and time-domain nonlinear distortion compensation in high-speed OFDM-IMDD LR-PON with high loss budget," Opt. Express **25**(5), 5044–5056 (2017).
13. L. Dai, B. Wang, Y. Yuan, S. Han, C. I, and Z. Wang, "Non-orthogonal multiple access for 5G: solutions, challenges, opportunities, and future research trends," IEEE Commun. Mag. **53**(9), 74–81 (2015).
14. Y. Saito, Y. Kishiyama, A. Benjebbour, T. Nakamura, A. Li, and K. Higuchi, "Non-Orthogonal Multiple Access (NOMA) for Cellular Future Radio Access," in *Proceedings of IEEE Conference on Vehicular Technology* (IEEE, 2013), pp. 1–5.
15. S. Zhang, X. Xu, Lei Lu, Y. Wu, G. He, and Yan Chen, "Sparse Code Multiple Access: an Energy Efficient Uplink Approach for 5G Wireless Systems," in *Proceedings of IEEE Global Communications Conference* (IEEE, 2015), pp. 4782–4787.
16. Z. Yang, C. Pan, W. Xu, and M. Chen, "Compressive Sensing-Based User Clustering for Downlink NOMA Systems With Decoding Power," IEEE Signal Process. Lett. **25**(5), 660–664 (2018).
17. Q. Wu, Z. Feng, M. Tang, X. Li, M. Luo, H. Zhou, S. Fu, and D. Liu, "Digital Domain Power Division Multiplexed Dual Polarization Coherent Optical OFDM Transmission," Sci. Rep. **8**(1), 15827 (2018).
18. B. Lin, W. Ye, X. Tang, and Z. Ghassemlooy, "Experimental demonstration of bidirectional NOMA-OFDMA visible light communications," Opt. Express **25**(4), 4348–4355 (2017).
19. B. Lin, X. Tang, Z. Zhou, C. Lin, and Z. Ghassemlooy, "Experimental demonstration of SCMA for visible light communications," Opt. Commun. **419**, 36–40 (2018).

Optics EXPRESS

20. H. Marshoud, V. M. Kapinas, G. K. Karagiannidis, and S. Muhaidat, "Non-orthogonal multiple access for visible light communications," IEEE Photonics Technol. Lett. **28**(1), 51–54 (2016).
21. X. Guan, Y. Hong, Q. Yang, and C. C.-K. Chan, "Non-orthogonal multiple access with phase pre-distortion in visible light communication," Opt. Express **24**(22), 25816–25823 (2016).
22. C. Chen, W.-D. Zhong, H. Yang, and P. Du, "On the Performance of MIMO-NOMA-Based Visible Light Communication Systems," IEEE Photonics Technol. Lett. **30**(4), 307–310 (2018).
23. B. Lin, Z. Ghassemlooy, X. Tang, Y. Li, and M. Zhang, "Experimental demonstration of an NOMA-PON with single carrier transmission," Opt. Commun. **396**, 66–70 (2017).
24. B. Lin, X. Tang, X. Shen, M. Zhang, C. Lin, and Z. Ghassemlooy, "Experimental demonstration of SCMA-OFDM for passive optical network," Opt. Fiber Technol. **39**, 1–4 (2017).
25. F. Lu, M. Xu, L. Cheng, J. Wang, and G. Chang, "Power Division Non-Orthogonal Multiple Access (NOMA) in Flexible Optical Access with Synchronized Downlink / Asynchronous Uplink," J. Lightwave Technol. **35**(19), 4145–4152 (2017).

212.219.26.5 {ts '2019-11-25 09:44:05'}